A MECHANISTIC INVESTIGATION OF SOOT PRECURSORS

S. H. Bauer[a] and P. M. Jeffers[b]

[a] Department of Chemistry, Baker Laboratory,

Cornell University, Ithaca, New York 14853-1301

[b] Department of Chemistry, SUNY-Cortland, Cortland, NY 13045

INTRODUCTION

Fuels with low H/C ratios are particularly prone to soot production during combustion; aromatic species generally (but not universally) do so more readily than aliphatics. It is now well recognized that "soot" is not a singular material. Besides characterizing the variety of soots with respect to composition, volatile content, and structure, extensive efforts have been devoted to determining conditions which promote the development of soot in flames and in internal combustion engines. Many studies have been reported on the effects of inhibitors; reviews abound (1). During the past decade chemical kinetics investigations have proliferated with the hope of unraveling the mechanisms for its generation, ultimately to permit control of the types and magnitudes of soot emissions. There is general agreement on species types which initiate condensed aromatic ring growth (2); there is still disagreement as to whether ions play a major role(3); there is overall agreement on the spacial distribution of PAH in flames, as measured mass spectrometrically (4); composition constraints on fuel/oxidizer ratios for the inception of sooting, and the temperature range in flames wherein soot appears are sufficiently well-defined (5).

In this report our objectives are: **A.** To call attention to the differences and the conceptual similarities between the sooting process and a <u>kinetic</u> model for nucleation/condensation. **B.** List the types of precursors required for sooting, and the underlying experimental basis. **C.** Present a minimal set of reactions, with rate constants, which model the observed time evolution of condensed molecular structures (soot precursors). This list must incorporate a repetitive growth cycle for continued condensation. As a minimum, the model must semiquantitatively reproduce observed delay times for the onset of condensation. **D.** Present qualitative spectral data which support **C.**

A. The characteristic kinetic features of a typical nucleation/condensation mechanism (6) are: (a) An initial binary association sequence which reaches steady state at some small number (n) (7):

$$A_1 + A_1 \underset{}{\overset{(A)}{\rightleftharpoons}} A_2 \qquad [k_1 \; ; \; k_{-1}]$$

$$- - - - - - - - - - - - - -$$

$$A_{n-1} + A_1 \rightleftharpoons A_n \qquad [k_{n-1} \; ; \; k_{-(n-1)}]$$

Note that at this stage the rates of association/condensation are nearly balanced for each step: $k_{n-1}(A_1) \approx k_{-(n-1)}$. No activation energies are involved; association is driven by a decrease in enthalpy; dissociation is favored by an almost equal $T\Delta S$ term. This is followed by (b),

$$A_n + A_1 \underset{\leftarrow}{\overset{k_n}{\rightarrow}} A_{n+1}$$

$$A_{n+1} + A_1 \underset{\leftarrow}{\overset{k_{n+1}}{\rightarrow}} A_{n+2}$$

wherein steady state is achieved by unidirectional flow, such that $k_{n+1} \approx k_n$, with insignificant reversibility. Here the enthalpy factor completely dominates. The magnitude of n at which this "switch-over" occurs characterizes the critical size nucleus.

The contrast with soot production from C/H fragments is striking. The initial lag is due to: (α_1) the rate of pyrolysis of the fuel, to generate small reactive fragments, generally referred to as "acetylenic species", and (α_2) their partial recombination to [in some cases --- the direct production of] aromatic ring radicals; activation energies control these steps. Hence, minimal temperatures of ≈1500 K are required. It is likely that a dynamic local equilibrium similar to the steady state (a), develops between these small highly reactive radicals. When adequate levels of both types of species are attained, stage (β) follows; i.e. an essentially unidirectional growth sequence, wherein the acetylenic species add onto the aromatic radicals, in analogy with (b). Thus, there occurs a "switch-over" which has the appearance of a catastrophic onset of sooting. Since at all times in (β) the driving enthalpy for growth is countered by an opposing $T\Delta S$ term, at some higher temperature the latter quenches sooting (≈ 2100 K). This accounts for the bell-shaped generation profile [soot yield <u>vs</u> temperature] reported by many observers.

B. What are the essential precursors which operate in regions (α_1) and (α_2)? Observations, previously reported for shock tube pyrolysis studies of ten polycyclic aromatics (8), guided our choice of the smallest species which have to be incorporated in a minimal mechanism. For shock durations of <700 μs, over the temperature range 1500-2200 K, acetylene, tetramethylpentane, acenaphthene or acenaphthalene, when individually pyrolyzed, yielded insignificant amounts of soot. However, any aliphatic/aromatic combination under the same shock conditions produced copious amounts of soot. Clearly, two types of molecular species are required for the onset of sooting. It follows that one should anticipate longer delays when a single type is initially present because of the time required to generate the other type. Schematically,

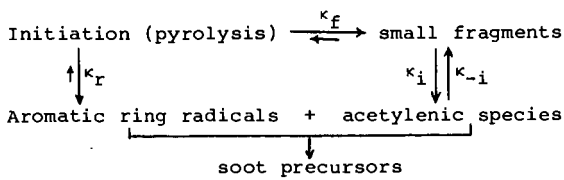

The relative magnitudes of κ_f and κ_r are determined by the structures of the fuel.

C. Two sets of reactions with appropriate rate constants are listed in Tables I and II, for benzene and toluene, respectively. We attempted to identify the smallest number of essential steps, not to list all reactions which plausibly occur concurrently with soot initiation.

C_6H_6: For the benzene pyrolysis our final set consists of 18 reactions with 18 H/C species (plus Ar), although at least twice that number of reactions and species [30] were considered during the preliminary calculations. Not included in Table I are intermediate radical stabilization steps.

We also treated the addition of acetylene as a single step:

$$C_6H_5 + C_2H_2 \rightarrow C_8H_5 + H_2;\ k_7 = 10^{13.7} \exp(-2000/RT)$$

rather than a two reaction sequence:

$$C_6H_5 + C_2H_2 \longrightarrow C_8H_6 + H;\quad k_7' = 10^{13}$$

$$C_8H_6 + \quad H \longrightarrow C_8H_5 + H_2;\ k_7'' = 2\text{x}10^{13} \exp(-6800/RT)$$

The typical growth cycle is illustrated by

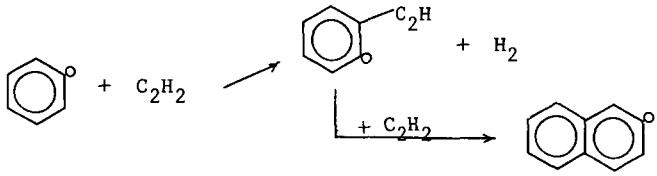

At each cycle one ring is added and a new radical is generated which repeats the cycle. As ring condensation proceeds there are possibilities for alternate routes to yield other observed products, for example R12; it was included because biphenyl is a commonly found product, although no further reactions of biphenyl occur other than the reverse of its formation. The other stable molecular products incorporated in this mechanism are C_2H_2, C_4H_2, $H_{10}C_{18}$, and $C_{22}H_{12}$. It is necessary to assign an upper limit to the largest species incorporated in the computer code; we chose $C_{22}H_{12}$ which serves as a "sink". Tests show that the concentration/time patterns for the last three species, for any selected terminus, remains essentially unchanged when the largest assumed unit was varied [$C_{18} \rightarrow C_{20} \rightarrow C_{22}$]. Clearly, the two-step growth sequence continues until the system is quenched.

Kinetic calculations, to model rates of production of soot precursors by pyrolysis, were performed with the Mitchell/Kee (9) shock kinetics program. All reactions were considered reversible, with their reverse rate constants calculated within the program by reflection through their equilibrium constants. Most of the unavailable thermodynamic parameters were estimated by Benson's group contribution recipe.

Figure 1 is a plot of the computed concentration-time profiles for 1% C_6H_6 in argon, reflected shock heated to 2120 K (initial). It shows the expected general features. During early times the mole fractions of H, C_2H_2, C_4H_2 and H_2 rise, that of C_6H_6 slowly declines and nearly steady state concentrations of C_6H_5 and C_8H_5 develop. The higher molecular weight products then slowly begin to grow, in sequence of increasing carbon content. The time dependence of the imposed cut-off at C_{22} provides a measure of the delay time for the onset of avalanche soot growth. Note that after a gradual decline, C_6H_6 drops sharply as do all the heavier species even though all reactions

were treated reversibly. $C_{22}H_{12}$ (the terminal species) increases (designated as the soot initiator). Eventually, after the lower carbon content species had passed through maximum levels, C_2H_2, C_4's and H_2 dominate.

A measure of the sensitivity of this mechanism to the rate constant for initiation (R1) was obtained by using a value derived by reflection of Frenklach's (1) estimate for the reverse of R1, 1×10^{13} mole/cc-sec, whereas the curves in Fig. 1 were calculated with k_1 about a factor of ten larger, as suggested by M. C. Lin (10); it is very close to the value reported by Fujii and Asaba (11). A faster initiation rate results, with a much earlier appearance of heavy products and considerably more extensive (eventual) destruction of benzene. When the one step phenyl radical decomposition (R5) was replaced by the sequence:

$$C_6H_5 \longrightarrow H_5C_6 \text{ (linear)} \; ; \quad k_4' = 2.4\times10^{12} \exp(-58{,}800/RT)$$

$$H_5C_6 \longrightarrow C_4H_3 + C_2H_2 \; ; \quad k_4'' = 1.8\times10^{15} \exp(-40{,}000/RT)$$

a dramatically slower depletion of all the low molecular species was indicated. This merits further investigation, possibly by direct assay of the time dependence for appearance of C_4H_3.

The proposed mechanism is sensitive to one more feature --- the initial concentration of C_2H_2. If one starts a calculation, as for Fig. 1, but with added C_2H_2 (mole fraction of 0.005), <u>the production of all the heavy products is strongly accelerated</u>. This accounts for our observations that soot formation from acenaphthene or acenaphthalene is significantly accelerated when C_2H_2 [or tetramethylpentane, which readily produces C_2H_2] was included in the initial mixture.

Two variations of the mechanism were found to exert a moderate effects on the rate of heavy product formation. The C_2H_2 addition sequence <u>via</u> one step, rather than two steps, delays somewhat the appearance of the final product. Reducing the value of k_{12} by a factor of 100 makes at most a 15-20% change in heavy species mole fractions at 5 μsec, with slightly larger differences in $C_{12}H_{10}$ and C_8H_6 concentrations at earlier times.

Finally, several factors were found to have slight or negligible effects. These non-critical factors include deletion of radical stabilization steps, incorporating an initial [artificially] high H atom concentration, the value for k_7 [acetylene addition to phenyl], and the inclusion of an alternate initiation process:

$$H + C_6H_6 \longrightarrow C_6H_7; \qquad k_1' = 4.5\times10^{14} \exp(-4300/RT)$$

$$C_6H_7 \longrightarrow C_4H_5 + C_2H_2; \quad k_1'' = 6 \times 10^{14} \exp(-92{,}000/RT)$$

Reduction of E_a from 92 to 80 kcal/mole for the second step had no effect. Substituting the bimolecular reaction:

$$C_6H_6 + C_6H_6 \longrightarrow C_6H_5 + C_6H_7 \; ; \quad k_1'' = (5\times10^{12}-5\times10^{16}) \exp(-85{,}000/RT)$$

for R1 failed to provide sufficient radical species for the pyrolysis sequence to proceed.

$C_6H_5CH_3$: The adequacy of our minimalist approach to develop a mechanism for the precursor stage of sooting is illustrated by the analysis of our shock tube data for toluene. The initiation steps (Table II) differ from those for benzene (steps 1-6, Table I) but thereafter the growth sequences are the same. Here also the calculated and observed delay times are in acceptable agreement. Six additional species must be included (C_7H_8; C_7H_7; C_3H_3; CH_3; CH_4 and C_2H_6). Reactions T 1, 2, 4, 5 and 6 were taken from Mizerka and Kiefer (12). The combined effect of reactions T2, T3, and T8 is to generate rapidly significant concentrations of C_6H_5 and C_6H_6. No effort was made to determine which reaction path is most effective. At temperatures around 1800°K and higher T2 is a significant pathway for the initial breakup of toluene. The rate constant for T3 was assumed to be (1/4) that for T4, and both are exothermic. T7 is a reasonable sink for CH_3 radicals, while the recombination of C_3H_3's [T8] maintains the reaction sequence alive in a simple fashion. All the initially estimated rate constants were used in the calculations without subsequent adjustments. The possibility that there are steps in the sequence T 1→8 which are not essential for the "minimal" mechanism was not fully tested; it appears that T7 could be dropped.

Our conclusion is that a few additional steps added to the simplified mechanism proposed for benzene, can account in a quantitative way for many features of the pyrolysis of aromatics, in general. For soot production, the major pathways are evident and inherently reasonable.

D. What experimental evidence exists, or can be developed, to support the above proposals? Other than direct mass spectrometric detection of PAH, one must look for some in situ diagnostic technique. Absorption and fluorescence spectra (5) are indicated, but there are obvious limitations. The samples consist of complex brews, characterized by superposed broad spectral bands. Thus, there is little likelihood that one could identify specific species. But, we are concerned with molecular types; the saving feature is the absence of oxygen or nitrogen chromophoric structures. The recorded spectra in the near uv, visible and down to the near infrared must arise from condensed polycyclic aromatics, either the stable species, as reported in the literature (12) or their radicals. To distinguish between general turbidity and characteristic absorptions, one should measure the temporal wavelength dependence of light loss on passage through the reacting medium, and its dependence on temperature. Also, a condition for the adequacy of a minimal mechanism is that it correctly predict the temperature dependence of the time delays of the growth of condensed polycyclic aromatics.

EXPERIMENTAL

Since a large diameter shock tube was not available to measure the time dependent spectra tranverse to the shock flow, we had to resort to recording integrated absorption spectra by passing the probing beam axially along the shock direction. The data were resolved by imposing an additional integration step in the analysis. A 1" I.D. stainless steel shock tube (Fig. 2a) was fitted with a clear plastic end-wall at the driver section; a quartz window and filter terminated the test section. A He/Ne laser beam (6328 Å), directed along the axis of the tube, was aimed at a small aperture inserted between the quartz end plate and the narrow band pass filter. The phototube output was recorded simultaneously with the output of two pressure trans-

ducers located 1 cm and 11 cm from the downstream end. In later experiments the laser was replaced by a Xe lamp and the phototube by a monochromator/linear array of diodes for scanning other regions of the spectrum (Fig. 2b).

The signals from the piezo-gauges allow evaluation of the shock speed and dwell time. Since the gas at different initial positions along the tube is heated for different lengths of time, the extent of light absorption (or scattering) must be integrated along the entire tube length. Let $A_n(x;t')$ be the instantaneous concentration of the $n^{\underline{th}}$ absorbing species, where $t' = t_w - x/u_r$; t_w is the laboratory time for shock reflection at the quartz window, x is the return distance from the window at the location of the reflected shock, and u_r the reflected shock speed. Then, the recorded light loss is:

$$I^{\lambda}(t')/I_o^{\lambda} = \exp\left[-\sum_n \mu_n(\lambda,T_5) \int_o^{u_r t'} A_n(t_w - x/u_r)dx\right] . \qquad [1]$$

Here we assumed that no chemical processing and no absorption (at the probing wavelength) occurs during the incident shock.

Reflected shock temperatures ranged from 1400°K to 2200°K, and were controlled by varying both the initial pressure of the test gas and the diaphragm thickness. Residence times were generally about 700 μsec, followed by a rapid quench due to expansion. Analysis by g.c. of the shock heated samples (both gas phase and condensable species) indicated that during the test time the products had not achieved their equilibrium concentrations at the reflected shock temperatures.

I. The molecular species which strongly absorb red light (He/Ne) appear after an extended induction period which is temperature dependent. [Typical shapes are illustrated by the curves in Fig. 3b.] In turn, these absorbers are removed by continued condensation. Hence the initial flattening and the subsequent slow growth of absorption. We noted that substantial light loss occurred even in some cases where little soot was produced. Curves of $\ln(I/I_0)$ vs t (corrected for emission) were sigmoidal and often saturated at $I>0$. We presume that the recorded light loss was due primarily to absorption by transient species, which are precursors of soot particles, and to a lesser extent by soot, which forms during the later stages of the experiment. The absorbing species at λ6328 must be condensed ring entities, such as the para sequence of the acene series (12), and/or radicals of similar structure (Fig. 4). For the 2% runs, the concentration-time profiles for $C_{20}H_{11}$ [designated as the representative absorber of λ6328] were integrated, per eq. [1]. These curves show all the salient features of the recorded (I/I_0) traces, i.e. the sigmoid shape following a delay, a relatively sharp rise and a slow approach to saturation. The computed times selected for minimal detection of absorption (at 3x noise level) check quite well with the measured values (Table III).

II. Absorption curves over a range of wavelengths (400-800 nm) were obtained with the second experimental configuration (Fig. 2b). Typical time/wavelength spectra at two extremes are shown in Fig. 3a and Fig. 3b. No significant differences appear over a spectral range of 20 nm. However, there are clear, significant differences between the spectral scans at 811 and 392 nm. First, the delay times are shorter and the rise times are faster for the same shock speeds, indicating more rapid rates for generating the smaller species which absorbed

near the uv, compared with the much longer delay times for the appearance of the larger species, which absorb in the near infrared. Second, a two step process appears at 800 nm, where the initial relatively fast rise is followed by a slower continued increase in absorption, demonstrating subsequent growth, since the absorption edge continues to move toward the longer wavelength.

Two types of information are presented by these plots (recorded at 100 nm intervals, 400-800 nm); delay times (t_i) which measure induction times for the development of absorbing species, and rise times $[(t_f-t_i)/2]$, which are mean inverse rates of production of these species. For any specified shock temperature (T_5), a plot of t_i vs mean λ has a positive slope, as expected for a sequential growth of absorbers with leading edges progressing toward the red. For any specified λ, t_i is longer the lower the shock speed (T_5).

Because of the restricted range of final densities covered in these experiments, the half-times for attaining the first saturation level do not permit us to determine whether the global process is first or second order. However, graphs of $\ln k_u \equiv 10^6 \ln 2/t_{1/2}, \mu s)$ vs $1/T_5$ (Fig. 5) clearly show nesting of points for the sequence of λ's, as expected, assuming that the leading edges of the absorption curves measure the larger units at longer wavelengths. At any T_5, the k_u's are consistently larger when derived from 400 nm traces compared with 800 nm traces.

ACKNOWLEDGMENTS

This program was supported by the U. S. Department of Energy under contract DE-AC01-80 ER 10661.A004. We sincerely thank Dr. R. J. Kee for copies of the Sandia computer codes, Professor C. F. Wilcox, Jr. for extensive discussions of the possibilities and limitations of the Diels-Alder addition sequence, and Professor J. H. Kiefer for discussions of his shock tube pyrolysis experiments of toluene and ethylbenzene.

REFERENCES

1. Sections on SOOT & COMBUSTION GENERATED PARTICULATES can be found in every Symposium (International) on Combustion [Combustion Institute], starting with the 15th (1974) through the 21st (1986). Also: Wagner, H. Gg., 17th Symposium (International) on Combustion, The Combustion Institute, Pittsburgh, **1978**, p. 3; Haynes, B. S. and Wagner, H. Gg., Prog. Energy Comb. Sci. **1981**, 7, 229.

2. Frenklach, M., Clary, D. C., Gardiner, W. C. and Stein, S. E., 20th Symposium (International) on Combustion, The Combustion Institute, Pittsburgh, **1984**, p. 887; Bockhorn, H., Fetting, F. and Wenz, H., Ber. Bunsenges. Phys. Chem. **1983**, 87, 1067; Homan, K. H., 20th Symposium (International) on Combustion, The Combustion Institute, Pittsburgh, **1984**, p. 857.

3. Keil, D. G., Gill, R. J., Olson, D. B. and Calcotte, H. F., 20th Symposium (International) on Combustion, The Combustion Institute, Pittsburgh, **1984**, p. 1129 -- favor ionic mechanisms; Bertrand, C. and Delfan, J-L., Comb. Sci. and Tech. **1985**, 44, 25; discount significant contributions from ions.

4. Longwell, J. P., 19th Symposium (International) on Combustion, The Combustion Institute, Pittsburgh, 1982, p.1339.

5. Smith, K. C., et al., Comb. and Flame, 1985, 62, 157; Frenklach, M., Hsu, J. P., Miller, D. L. and Matula, R. A., Comb. and Flame, 1986, 64, 141.

6. Bauer, S. H. and Frurip, D. J., J. Phys. Chem. 1977, 81, 1015.

7. Bauer, S.H., Wilcox, C.F., Jr. and Russo, S., J. Phys. Chem. 1978, 82, 59.

8. Bauer, S. H. and Zhang, L-M., 14th International Symposium on Shock Tubes and Waves, Ed. R. D. Archer and B. E. Melton, New S.W. University Press, 1983, p. 654.

9. Mitchell, R. E. and Kee, R. J., Sandia National Laboratories, Livermore, CA, SAND-82-8205 (March, 1982).

10. Hsu, D. S. Y., Lin, C. Y. and Lin, M. C., 20th Symposium (International) on Combustion, August 1984. See also: Kieffer, J. H., et al., J. Phys. Chem. 1985, 89, 2013.

11. Fujii, N. and Asaba, T., 14th Symposium (International) on Combustion, The Combustion Institute, p. 433 (1973).

12. Clar, E., Polycyclic Hydrocarbons, 1964, Academic Press, London; Clar, E., The Aromatic Sextet, 1972, J. Wiley & Sons, London; Stern, E. S. and Timmons, C. J., Electronic Absorption Spectroscopy in Organic Chemistry, 1970, Edward Arnold, London; Karcher, W., et al., Ed., Spectral Atlas of Polycyclic Aromatic Compounds, 1983, D. Reidel, Dorchester.

TABLE I

	MINIMAL MECHANISM (C_6H_6)	log A	E_0(cal mole^{-1})	Ref.
1.	$C_6H_6 = C_6H_5 + H$	15.7	108000.	10
2.	$C_2H + C_6H_6 = C_6H_5 + C_2H_2$	13.3	0.00	2
3.	$C_2H_2 + C_2H_2 = C_4H_3 + H$	12.3	65000.	a
4.	$C_6H_5 = C_4H_3 + C_2H_2$	14.8	82800.	b
5.	$C_4H_3 = C_2H_2 + C_2H$	10.76	52500.	2
6.	$C_4H_3 + Ar = Ar + C_4H_2 + H$	16.0	45000.	c
7.	$C_6H_5 + C_2H_2 = C_8H_5 + H_2$	13.7	2000.0	2
8.	$C_8H_5 + C_2H_2 = C_{10}H_7$	13.0	0.00	2
9.	$C_{10}H_7 + C_2H_2 = C_{12}H_7 + H_2$	13.0	2000.0	2
10.	$C_{12}H_7 + C_2H_2 = C_{14}H_9$	13.0	0.00	2
11.	$C_{14}H_9 + C_2H_2 = C_{16}H_9 + H_2$	13.0	2000.0	2
12.	$C_6H_5 + C_6H_6 = C_{12}H_{10} + H$	11.0	11000.	d
13.	$C_{16}H_9 + C_2H_2 = H_{10}C_{18} + H$	12.74	10000.	e
14.	$C_{16}H_9 + C_2H_2 = C_{18}H_9 H_2$	13.0	2000.0	2
15.	$C_{18}H_9 + C_2H_2 = C_{20}H_{11}$	13.0	0.00	2
16.	$C_{20}H_{11} + C_2H_2 = C_{22}H_{12} + H$	12.74	10000.	e
17.	$H_2 + Ar = H + H + Ar$	$(12.08)T^{1/2}$	92600.	
18.	$C_6H_6 + H = C_6H_5 + H_2$	13.3	6600.	c

Footnotes for TABLE I

a. J. Warnatz, Ber. Bunsenfesell. Phys. Chem. **1983**, 87, 1008 but $E_0 = \Delta H_{reaction} = 67.4$ kcal mole^{-1} (rather than 54 kcal mole^{-1}).

b. T. Asaba and N. Fujii, 13th Symposium (International) on Combustion, The Combustion Institute, Pittsburgh (**1971**), p.155.

c. Values of A are those given in (2), but with selected E_0's.

d. A slightly adjusted value based on --- C. T. Brooks, S. J. Peacock and B. G. Renber, J. Chem. Soc. Farad. Trans. I, **1979**, 75, 652 and ref. (b).

e. Based on the reaction:

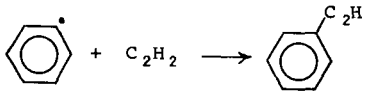

$k = 10^{13}$

For (13) and (16) we assumed a somewhat lower A value and inserted $E_0 \approx 10$ kcal mole^{-1}, because in these the H atom is lost from the ring rather than from the added moity (C_2H_2).

TABLE II
Initiation Steps for Toluene

	MINIMAL MECHANISM ($C_6H_5CH_3$)	log A	E_0 (cal mole^{-1})	Ref.
T1	$C_7H_8 = C_7H_7 + H$	12.9	72,600	9
T2	$C_7H_8 = C_6H_5 + CH_3$	11.6	90,000	9
T3	$H + C_7H_8 = C_6H_5 + CH_4$	1+ 4log T	2,100	estimated
T4	$H + C_7H_8 = C_7H_7 + H_2$	1.6+ 4log T	2,100	9
T5	$C_7H_7 = C_3H_3 + 2C_2H_2$	14.0	84,800	9
T6	$C_7H_7 + H = C_3H_3 + C_4H_3 + H_2$	14.65	80,000	9
T7	$C_2H_6 + Ar = 2CH_3 + Ar$	14.6	88,400	estimated
T8	$C_3H_3 + C_3H_3 = C_6H_6$	13.0	-	estimated

TABLE III
Experimental Condition for Representative Shocks

Composition	p_1 (Torr)	u_1 (mm/μsec)	T_5(°K)	$\rho_5 \times 10^3$ (g/cc)	Exp'tl Δt(μsec)	Calc Δt(μsec)
2.0% toluene	110	.893	1612	1.93	340	320
"	95	.943	1700	1.64	100	
"	85	.962	1725	1.82	70	
"	65	1.02	1812	1.37	40	50
2.0% benzene	85	.926	1767	1.41	240	240
"	95	.926	1767	1.55	380	
"	85	.926	1767	1.41	360	
"	65	.980	1910	1.51	50	60
"	65	1.00	1950	1.56	50	40

p_1(Torr): total pressure of fuel plus Ar; Δt(μsec) is interval between the onset of the reflected shock and the toe of the absorption trace.

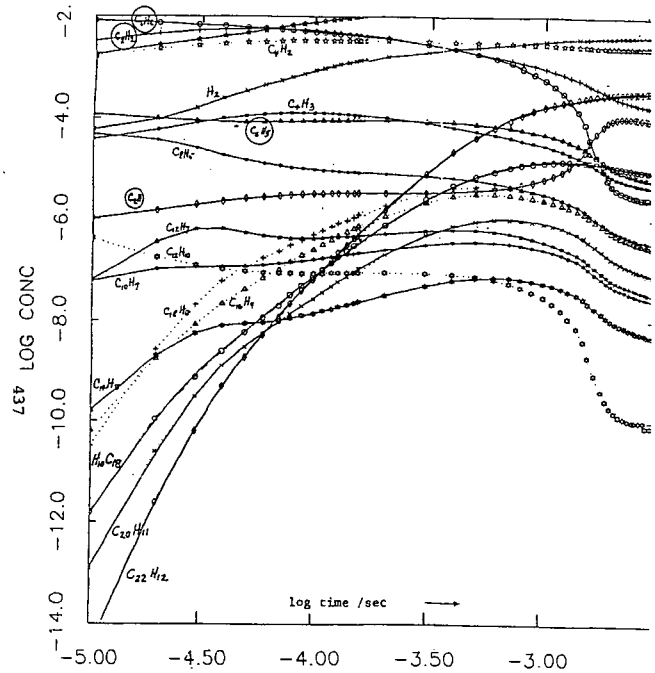

Figure 1. Calculated dependence of mole fraction on time, of various species, for shock heated 1% benzene in argon. T_5(initial) = 2120K; T_5(final) = 1907K.

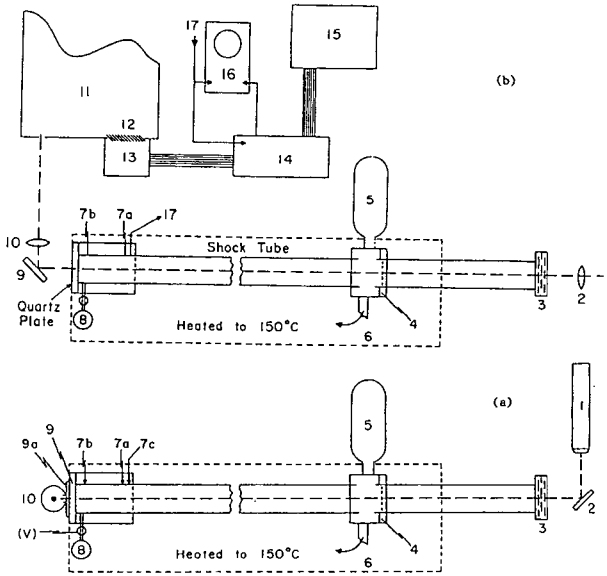

Figure 2. Schematic of shock tube and optical configuration.
(a) 1.He/Ne laser; 2.Mirror; 3.Plastic back-plate.
4. Diaphragm location; 5.Quench tank; 6. Lead to vacuum lines
7. Piezo gauges (a,b); 7c. Piezo crystal to trigger;
8. Sampling port; 9. Quartz window; 9a. Optical filter;
10. Phototube.
(b) 10. Lens; 11. Monochromator; 12. Linear array detectors;
13. Amplifiers and digitizers;14.Read and hold; 15.Computer.

Figure 3. Absorption spectra of shock heated toluene (2% in Ar); reflected shock regime. All spectra were recorded with 20 μs resolution. t_r=0 indicates the time when the incident shock was reflected from the quartz end plate.
(a) Incident shock speed u_i=1.031 mm/μs. Compare the delay times and absorption rise times for 400nm, with
(b) Incident shock speed u_i=1.020 mm/μs, of spectra at 800 nm.

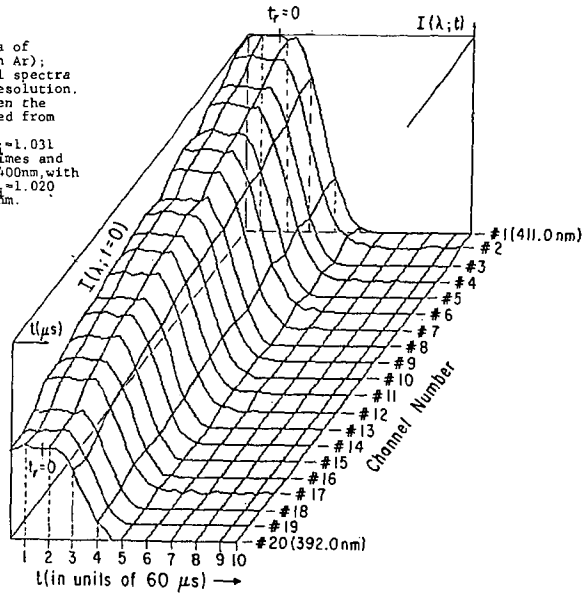

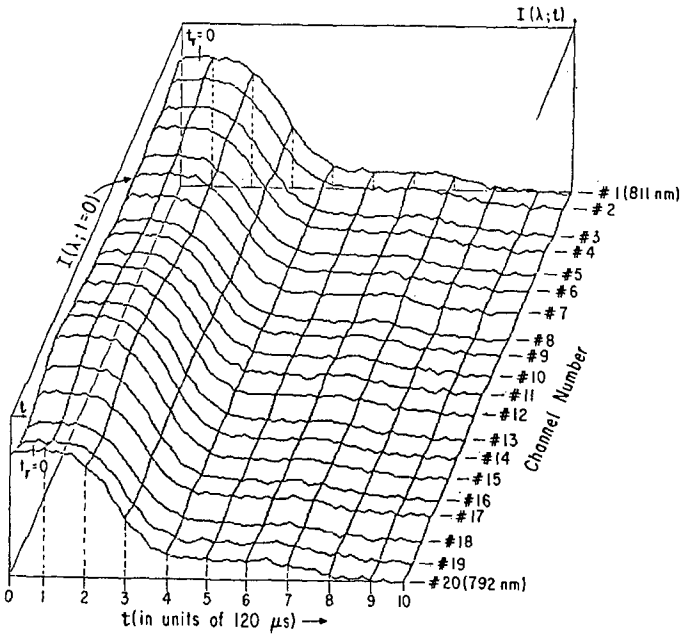

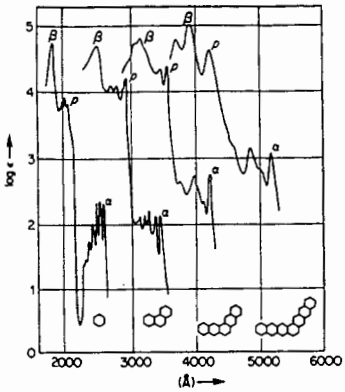

Figure 4. Absorption spectra in the phene series

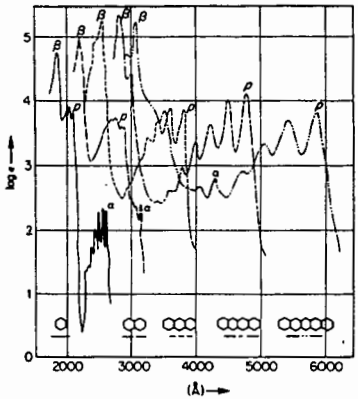

Absorption spectra of the acene series

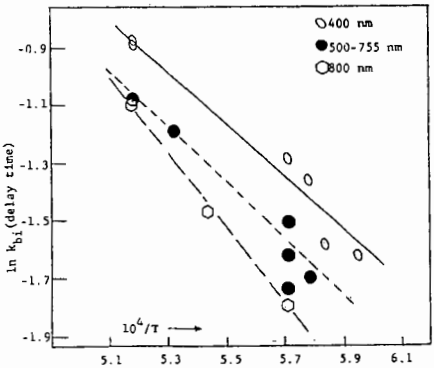

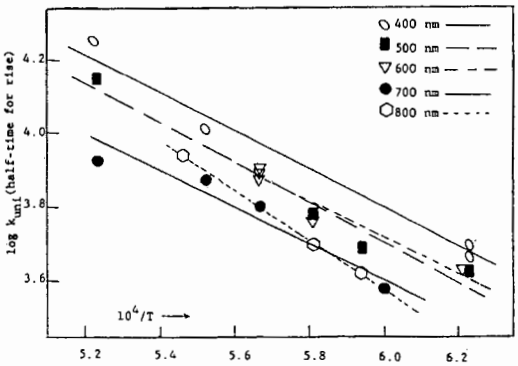

Figure 5a. The delay time for onset of absorption is the reciprocal of a mean bimolecular rate constant (arbitrary units) which decreases with the size of the absorbing units. The largest absorbers (at 800 nm) require a larger activation energy.

Figure 5b. The mean half-times for generating the larger absorbers increases with increasing size. The 800 nm absorbers require a larger activation energy (≈30 kcal/mole) compared to those which absorb at 400nm (≈24 kcal/mole).